Atmos. Chem. Phys. Discuss., 11, 15775–15799, 2011
www.atmos-chem-phys-discuss.net/11/15775/2011/
doi:10.5194/acpd-11-15775-2011

Atmospheric Chemistry and Physics Discussions

Optical properties, morphology and elemental chemical composition of atmospheric particles at T1 supersite on MILAGRO campaign

G. Carabali[1], R. Mamani-Paco[1], T. Castro[1], O. Peralta[1], E. Herrera[2], and B. Trujillo[2]

[1]Centro de Ciencias de la Atmósfera, UNAM, México
[2]Centro de Investigaciones de Materiales Avanzados, Chihuahua, México

Received: 4 April 2011 – Accepted: 12 May 2011 – Published: 25 May 2011

Correspondence to: T. Castro (telma@atmosfera.unam.mx)

Published by Copernicus Publications on behalf of the European Geosciences Union.

Abstract

Atmospheric particles were sampled at T1 supersite (19°43′ N latitude, 98°58′ W longitude, and 2340 m above sea level) during MILAGRO campaign. T1 was located at the north of Mexico City Metropolitan Area (MCMA). Aerosol sampling was done by placing transmission electron microscope (TEM) copper grids on the last 5 stages of an 8-stage MOUDI cascade impactor (d_{50} = 1.8, 1.0, 0.56, 0.32, and 0.18 µm). Samples were obtained at morning (06:00–09:00), noon (11:00–14:00), afternoon (16:00–19:00) and evening (21:00–24:00) local time. Absorption and scattering coefficients, and particles concentration (0.01–3 µm aerodynamic diameter) were measured simultaneously using a PASP absorption photometer (operated at 550 nm), a portable integrating nephelometer (at 530 nm) and a CNI particle counter. TEM images of particles were acquired at different magnifications using a CM 200 Phillips TEM-EDAX system.

The morphology of atmospheric particles for two aerodynamic diameters (0.18 and 1.8 µm) was compared using border-based fractal dimension. Particles sampled under Mexico City pollution influence showed not much variability, suggesting the presence of more compact particles in smaller sizes (d_{50} = 1.8 µm) at the site. The presence of higher numbers of compact particles can be attributed to aerosol aging and secondary aerosol formation, among others. Under early morning conditions, smaller particles (d_{50} = 0.18 µm) had more irregular features resulting in a higher average fractal dimension. Energy dispersive X-ray spectroscopy (EDS) was used to determine the elemental composition of particles. EDS analysis in particles with d_{50} = 0.18 µm showed a higher content of carbonaceous material and relevant amounts of Si, Fe, K, and Co. This may indicate an impact from industrial and vehicle's emissions on atmospheric particles.

ACPD

11, 15775–15799, 2011

1 Introduction

Most megacities in the developing world lie in subtropical and tropical latitudes, with a population growth so intensive that urban areas are constantly increasing without adequate planning. Mexico City is one of those, along with its altitude 2240 m a.s.l. (meters above sea level) it has meteorology and chemistry that are quite different from other megacities at midlatitudes. Raga et al. (2001) reported high solar irradiance, light winds and different atmospheric removal processes. But, this situation is moreover complicated by the plumes from the Popocatepetl volcano, a natural source of gases and sulfate enriched aerosols. During volcanic activity the plumes contain significant quantities of aerosols composed by sulfates, especially in the smaller sizes (Jimenez et al., 2004).

Another aerosol component, black carbon (BC), absorbs solar radiation and can be present in atmospheric particles in a number of mixing states, for instance: different from other aerosol particle components (externally mixed), included with them (internally mixed), or having a black carbon core that could be enclosed in a well-mixed shell.

As particles age, inorganic (i.e. nitrates and sulfates) and organic species coat them. Also, it seems that humidity influences the amount of sulfates present in particles. In days with high relative humidity a larger fraction of sulfates is reported (Baumgardner et al., 2000).

In Mexico City, the light absorbing in atmospheric aerosols is mainly due to particles from motor vehicles exhausts, especially diesel engines (Molina and Molina, 2002). In the mornings there are fresh particle emissions with high BC contents, which along the day get coated by secondary organics (Salcedo et al., 2006); Paredes-Miranda et al., 2009) contributing also to decrease particle single scattering albedo.

The optical properties also depend on the internal distribution of chemical species that make up the particles, if they are mixed in internal, external or a core shell structure. For example, the absorption coefficient of black carbon mixed with non-absorbent

ACPD
11, 15775–15799, 2011

particles is larger for an internal mixture than for an external mixture (Horvath et al., 1993).

Many studies on morphology and chemical composition (Dye et al., 2000; Xiong and Friedlander, 2001; Katrinak et al., 1993; Okada and Heintzenberg, 2003) report different shapes of atmospheric particles (spheres, aggregates, and irregularly shape) using electron microscopy.

On these studies it has been possible to classify particles based on a basic elemental composition and on morphology. Some authors (Mogo et al., 2005; Li and Shao, 2009) classified atmospheric particles into the following groups: mineral, Ca-S, S-rich, K-rich, organic, soot, fly ash, and metal.

In this research we place a MOUDI impactor to sample atmospheric particles at T1 supersite during MILAGRO campaign (Molina et al., 2010) and observed the morphology of individual particles with a transmission electronic microscope (TEM), and then calculate their fractal dimensions (D_f), also getting information about the elemental chemical composition for some of them. We compared two sampling days, one of them with influence (19 March) of pollution plumes from Mexico City, and the other one without influence (15 March).

Also, we only concentrate on those particles with 1.8 and 0.18 µm aerodynamic diameters. The fractal dimension for particles wrapped in these sizes tends to be more sensitive to changes in ambient weather conditions (Mamani-Paco, 2004).

2 Experimental method

2.1 Aerosol particles sampling

T1 was located at the *Universidad Tecnológica de Tecamac*, State of Mexico, with coordinates 19°43′ N latitude and 98°58′ W longitude, at 2340 m a.s.l. altitude. The site was towards the north of Mexico City Metropolitan Area (MCMA), and represents a place where emissions are fresh and well mixed (Molina et al., 2010).

ACPD
11, 15775–15799, 2011

From 1 to 31 March, we placed a particle soot/absorption photometer (PSAP) operated at $\lambda = 565$ nm, a nephelometer model M903 operated at $\lambda = 530$ nm (both from Radiance Research, Inc.) to measure optical properties of particles. Both instruments were connected to a particle counter (CPC) model 3010 (TSI, Inc.), which measured particles concentrations within 0.01–3 µm diameter range. The sampling system was 4 m above the ground level.

Also, we used two eight-stage micro orifice uniform deposit impactors (MOUDI) model MSP 100 to collect atmospheric particles with different aerodynamic diameters every two days, during March. On the last 5 stages ($d_{50} = 1.8$ µm, 1.0 µm, 0.56 µm, 0.32 µm, and 0.18 µm) of the MOUDI impactor we placed transmission electron microscope (TEM) grids (Cu).

Particle sampling schedules were established for early morning (06:00–09:00), noon (11:00–14:00), afternoon (16:00–19:00), and evening (21:00–24:00) local time. Also, model MM5 predictions for the campaign (de Foy, 2006) and meteorological data for T1 provided the wind direction prevailing from the Mexico City, showing the days with and without a clear influence of pollutants to take samples with the impactor.

2.2 TEM micrographics and elemental chemical analysis of atmospheric particles

CM 200 Phillips TEM-EDAX system provided TEM images of particles at different magnifications. We analyzed the morphology of particles with digital TEM images and classified their shape based on their fractal dimension (D_f). TEM provided high resolution images for particles and the EDS technique gave information about their elemental chemical composition.

With the images we calculated fractal dimensions for more than 30 individual particles per TEM grid, based on their perimeter (Kindratenko et al., 1994), sampled every two days from 1 to 19 March (at T1), and 27 March (at T0).

More than 2500 TEM images were taken, but we calculated fractal parameters for about 500 particles. With the fractal dimensions, sorted by sizes and sampling times

ACPD
11, 15775–15799, 2011

of the day, we tried to collect enough evidence of aerosol aging process along the day. Dye et al. (2000) and Kidratenko (1994) have observed the aging behavior of aerosols with similar procedures.

3 Results

3.1 Meteorological conditions

The MM5 model (de Foy, 2006) and the meteorological data recorded at T1 supersite provided information about the days with or without influence from MCMA. We choose 15 and 19 March to compare results, because they are respectively days without or with influence from the pollution plume emitted at MCMA. On 15 March, wind direction at T1 prevails from the north, while on 19 March the wind prevails from the south, where the MCMA is located. It was assumed that the winds from the south carried pollutants from the urban area to the site. Also, samples obtained on those days were good for comparison. Figure 1 shows the time series (local time) for wind direction and speed on both days.

3.2 Optical properties of particles

Table 1 shows the average values for absorption (σ_{abs}) and scattering (σ_{sct}) coefficients obtained at T1, compared to other measurements done in a rural area at Pico de Orizaba (Marquez et al., 2005) and Mexico City (Baumgardner et al., 2007). Average values obtained at T1 for σ_{abs} were higher than those reported for Pico de Orizaba and Mexico City, but average values for σ_{sct} were between those measured at Pico de Orizaba and Mexico City.

Figure 2 shows time series for particle concentration, σ_{sct}, σ_{abs}, and single scattering albedo (SSA) on both days. On 15 March, early in the morning (07:00) local sources generated 50 000 particles per cubic centimeter within 0.01–3 μm diameter, and around

ACPD
11, 15775–15799, 2011

10:00 the concentration decreased to 10 000. There were also episodes from 18:00 to 24:00 where the particles concentrations increased and gradually arrived to 40 000. Temporary changes in meteorological conditions could cause a major accumulation of particles during morning and night. Cold winds coming from the north to T1 decreased temperatures, promoting a suitable condition to reduce height on the mixed layer. On 19 March, particles concentration increased gradually from 09:00 to 13:00 when the plume of pollutants from MCMA arrived to T1, and decreased around 22:00 when the pollution activities ceased at Mexico City. The little increase in particles number concentration on 19 March also may result from diluted plumes arriving from Mexico City two days before (de Foy, 2006).

Scattering coefficient on 15 March increased again early in the morning and after 19:00, but decreased during 12:00 to 18:00. However, on 19 March the σ_{scat} fell down to 40 Mm^{-1} at 10:00, when the particles concentration increased. After 13:00 the scattering increased and finally at 19:00 the values remained at 30 Mm^{-1}. The higher scattering values at midday perhaps are caused by the presence of mixed aerosols. That day was characterized by the influence of the plume of pollutants from MCMA. So, the σ_{sct} suggest that particles could have a complex chemical composition that improved the scattering of light.

Episodes with high values on absorption coefficient occurred along the mornings and nights. Perhaps, they are caused by vehicular emissions. However, those from 15 March are higher (without the influence from Mexico City pollution) than the values from 19 March (influenced from Mexico City). Absorption coefficients of particles measured on 15 March maybe indicate an influence of local sources. Bond et al. (1999) suggest that the absorption of an old aerosol is approximately 1.5 times greater than a fresh emission.

Figure 2 also shows the single-scattering albedo (SSA) calculated on both days. 15 March was affected by north winds (from Golf of Mexico) and that day had a relative clean atmospheric background and the SSA showed two main maximums values at 0.74 and 0.81. Doran et al. (2007) reported similar values measured at T1 during

ACPD
11, 15775–15799, 2011

daytime, using a multi filter rotating shadow band radiometer. The SSA had a little increase on 19 March, with 0.77 average values, indicating perhaps that the pollutants plume transported aged particles to T1.

The minima values of SSA on 19 March are mainly attributed to the presence of black (EC) and organic carbon (OC) on atmospheric particles. Both species have a strong diurnal variation; their concentration increase during the nighttime and increase on the morning (Doran et al., 2007).

3.3 Particle morphology

Figure 3 shows TEM images for particles with different sizes sampled at T1. Particle diameter corresponds to the nominal aerodynamic diameters on MOUDI. All particles are irregularly shaped and it is not easy to assign a structure to the naked eye. Figure 4 shows particles with different shapes (some more irregular than others); the arrow points to their main structure, which is composed of tiny spherules forming aggregates. This is the typical structure present in carbonaceous material originated in combustion processes. Particles are crowded together and are more compacts resulting in two mixed states: external and internal.

Figure 4 shows particles with $d_{50} = 0.18$ sampled at T1 on different sampling times. Complex morphology of particles can be noticed and soot chains are seen attached to other rounded particles that should be sulfates. Soot particles look like they are internally mixed.

Our sampling technique (TEM grids into last MOUDI stages), classified particles by aerodynamic diameter ranges and not always match with previous atmospheric particle morphology studies; however, it is possible to see agreements with fractal dimension scale reported by Dye et al. (2000).

Figure 4 shows images where particles have a round shape presenting fractal values close to 1.0, while the particles with complex shapes tend to have values near to $D_f = 2.0$. Soot particles are attached to other more compact units changing their morphology and evidencing aerosols aging processes.

ACPD
11, 15775–15799, 2011

The morphology for different particle sizes shows marked differences. In our study, it can be noted that particles with higher aerodynamic diameters tend to have a more spherical shape. Particles with lower aerodynamic diameters reflect the formation of soot with a characteristic irregular (fractal) shape (Kindratenko, 1994; Mamani-Paco, 2004). This may indicate different steps in aerosol aging processes; i.e. particles are released to the atmosphere as fractal ashes with voids, slowly as they age, by condensation or impactation the voids are filled and the shape becomes more rounded. These processes continue and particles increase in size which results in change of their morphology and other physical and chemical properties.

Particles analyzed from 15 March have fractal dimension (D_f) average values higher than those from 19 March. On 15 March, local emissions dominated, especially in the morning periods. But on 19 March there are more aged particles transported from other place. The daily evolution of σ_{abs}, σ_{scat} is affected by traffic hour patterns governed by environmental conditions. Similarly, fractal dimensions show variations associated to particles analyzed.

Frequency histograms (Figs. 5 and 6) indicate high number of particles with irregular shapes that perhaps are associated with fresh soot emissions (Dye, 2000) absorbing radiation efficiently and therefore are responsible for the absorption peak that appears early morning on both days.

The histograms of particles $d_{50} = 0.18\,\mu m$ on 19 March show that the fractal dimensions tend to 1.0 in the four sampling times, while the histograms for 15 March show a more even distribution of fractal dimensions. Table 2 presents the basic statistics for this particle size. For instance, average D_f for particles on 19 March at morning and noon (1.10±0.06 and 1.08±0.06) are lower than those for 15 March (1.15±0.08 and 1.09±0.06). The difference in the frequency histograms between samplings at morning 15 March and noon 19 March shows characteristic shapes for particles from fresh emissions and aging processes.

In particles with $d_{50} = 1.8\,\mu m$ there is no a definite pattern, except that in the morning and the evening of 19 March where the distribution of fractal dimension seems to

ACPD
11, 15775–15799, 2011

approach to 1.0. Another remarkable result is the fractal dimension distribution for 15 March at noon is centered on 1.06±0.03, and the distribution for 19 March is spread on other dimensions bins (1.08±0.05). Table 3 shows the basic statistic parameters for this particle size.

Fractal dimension histograms for 19 March show the abundance of particles with low values of D_f (more rounded particles), indicating the presence of aged particles. Assuming that the particles reached T1 transported into the plume of pollutants, maybe they are composed by sulfate-coated soot and other volatiles compounds, which favored the dispersion of radiation instead of absorption (Baumgardner, 2007). At night, particles have fractal dimension similar to that described for the morning. This is due to the influence of such factors that were presented in both periods, such as the increase in emission sources and meteorological conditions.

The average values for D_f at noon are lower than morning and evenings, the photochemical activity could facilitate processes of condensation making this more aged aerosol.

Particle fractal dimensions at night and morning show similar trends but the last has higher average values. Both periods have same weather conditions, but in the morning there are fresh particles generated by vehicular emissions, while at night most of the particles suffered aging processes along the day.

3.4 Elemental chemical composition of particles

EDS provides chemical elemental concentration with 99% precision detection. Calcium, Cl, Cu, Fe, K, Mg, and Si were detected on the samples analyzed by EDS. Table 4 presents averaged results on elemental chemical composition for particles showed on Fig. 3.

Elemental chemical analyses performed on some particles (i.e. Fig. 3) demonstrate aggregates with internal mixing. It is evident that the smallest aerodynamic diameter (d_{50} = 0.18 µm) has the highest percentage of elemental carbon, but also Fe and Co, in its structure. Last two elements could be released by local sources such as oxidation in

ACPD
11, 15775–15799, 2011

mechanical parts of cars, or metallurgical activities carried out near the area. In Mexico City fresh particulate emissions due to motor vehicle traffic, especially diesel engines are mostly carbonaceous with very low sulfur content (Molina and Molina, 2002), as it is illustrated on Table 4

Most soot particles observed in TEM are internally mixed with others composed by high levels of S and K. Spherical fly ash particles contain O, Si, and Al with minor proportion of Ca, Ti, Mn, and Fe (Fig. 3). Those elements are related to anthropogenic activities, like coal combustion for heating and some other industrial practices.

Particles with $d_{50} = 1.8\,\mu m$, have low oxygen and carbon percentages, but high levels of K (a biomass burning tracer) and other elements, such as Si, Na, Ca, and Al; which are more abundant in clayey soils and rocks (Seinfeld and Pandis, 1998). The elemental composition and morphology indicate that particles with sizes around 1.8 µm could be produced on agricultural activities that took place in areas nearby T1.

4 Conclusions

Average value of σ_{abs} at T1 is higher than those reported for Pico de Orizaba and Mexico City, and the average σ_{scat} is between that reported on those places. Marquez et al. (2005) report $\sigma_{abs} = 17\,Mm^{-1}$ and $\sigma_{scat} = 39\,Mm^{-1}$ average values at Pico de Orizaba and suggest that volcano fumes affects optical properties of particles originated in Mexico City and Puebla urban areas, located 250 and 90 km away, respectively.

Particles sampled under Mexico City pollution influence showed not much variability, suggesting the presence of more compact particles in smaller sizes ($d_{50} = 0.18\,\mu m$) at the site. The presence of higher numbers of compact particles can be attributed to aerosol aging and secondary aerosol formation, among others.

The combination of morphological and chemical information is not sufficient to identify the source of atmospheric particles. However, both are good tools to get information about the age of atmospheric particles sampled at T1, based on their shape. Ramsden and Shibaoka (1982); Pósfai et al. (2003); Kaegi and Holzer (2003); Li et al. (2003) use

ACPD
11, 15775–15799, 2011

similar analysis approach to study aerosol particles properties.

It is important to note that images and morphological information described in this article only correspond to non-volatile components of particulate matter. This is because the microscopy technique produces a vacuum loosing volatile compounds; also, under the electron beam some particles may change their shape (ammonium nitrate).

The mixed state of aerosol particles influences their absorption and scattering characteristics. It is believed that aerosols produced in Mexico City react to form particles with a complex chemical composition, and the presence of metals, Si and S, could be released by local sources causing a synergistic effect that change the scattering and absorption behavior of light, this is the case of soot inside a mixture of sulfates.

Elemental chemical composition analysis show different inclusions of inorganic elements grouped (S, K, and Si; Fe, Na, and P) which agree with previous studies in Mexico City. Sulfate inclusions and other components in aged soot particles are probably due to coagulation processes and collisions experienced by aerosols in the atmosphere of the sampling site which strongly affects the optical properties (Johnson et al., 2005; Marley et al., 2009; García et al., 2010).

Acknowledgements. The authors would like to thank the M. I. Saavedra for helping in the aerosols optical properties data analysis and gravimetric analysis. We want also to thank to L. Molina, J. Gaffney and S. Madronich for the facilities during MILAGRO campaign at T1. Also, we want to thank Dulce Nazareth Ramírez her help in editing the document.

References

Baumgardner, D., Raga, G. B., Kok, G. L., Ogren, J., Rosas, I., Baez, A., and Novakov, T.: On the evolution of aerosol properties at a mountain site above Mexico City, J. Geophys. Res., 105, 17, 22243–22253, 2000

Baumgardner, D., Kok, G. L., and Raga, G. B.: On the diurnal variability of particle properties related to light absorbing carbon in Mexico City, Atmos. Chem. Phys., 7, 2517–2526, doi:10.5194/acp-7-2517-2007, 2007.

ACPD

11, 15775–15799, 2011

Bond, T., Anderson, T. L., and Campbell, D.: Calibration and intercomparison of filter-based measurements of visible light absorption by aerosols. Aerosol. Sci. Technol., 30, 582–600, 1999.

De Foy, B., Varela, J. R., Molina, L. T., and Molina, M. J.: Rapid ventilation of the Mexico City basin and regional fate of the urban plume, Atmos. Chem. Phys., 6, 2321–2335, doi:10.5194/acp-6-2321-2006, 2006.

Doran, J. C., Barnard, J. C., Arnott, W. P., Cary, R., Coulter, R., Fast, J. D., Kassianov, E. I., Kleinman, L., Laulaien, N. S., Matin, T., Paredes-Miranda, G., Pekour, M. S., Shaw, W. J., Smith, D. F., Springston, S. R., and Yu, X. Y.: The T1-T2 study: evolution of aerosol properties downwind of Mexico City, Atmos. Chem. Phys., 7, 1585–1598, doi:10.5194/acp-7-1585-2007, 2007

Dye, A. L., Rhead, M. M., and Trier, C. J.: The Quantitative Morphology of Roadside and Background Urban Aerosol in Plymouth, UK. Atmos. Environ., 34, 3139–3148, 2000

García, L. Q., Castro, T., Saavedra, M. I., and Martínez-Arroyo, M. A.: Optical properties of aerosols: southern Mexico City. Atmósfera, 23, 4, 2010.

Horvath, H., Catalan, L., and Trier, A.: A study of the aerosol of Santiago de Chile III Light absorbing measurements, Atmos. Environ., 31, 3737–3744, 1997.

Jiménez, J. C., Raga, G. B., Baumgardner, D., Castro, T., Rosas, I., Báez, A.: On the composition of aerosol particles influenced by emissions of the volcano Popocatepetl in Mexico, Natural Hazards, 31, 21–37, 2004.

Johnson, K. S., Zuberi, B., Molina, L. T., Molina, M. J., Iedema, M. J., Cowin, J. P., Gaspar, D. J., Wang, C., and Laskin, A.: Processing of soot in an urban environment: Case study from the México City Metropolitan Area, Atmos. Chem. Phys., 5, 3033–3043, doi:10.5194/acp-5-3033-2005, 2005.

Kaegi, R. and Holzer, L.: Transfer of a single particle for combined ESEM and TEM analyses. Atmos. Environ., 37, 4353–4359, 2003.

Katrinak, K. A., Rez, P., Perkess, P. R., and Buseck, P. R.: Fractal geometry of carbonaceous aggregates from an urban aerosol, Environ. Sci. Technol., 27, 539–547, 1993.

Kindratenko, V. V., Van Espen, J. M., Treiger, B. A., and Van Grieken, R. E.: Fractal Dimensional Classification of Aerosol Particles y Computer-Controlled Scanning Electron Microscopy, Environ. Sci. Technol., 28, 2197–2202, 1994.

Li, J., Anderson, J. R., and Buseck, P. R.: TEM study of aerosol particles from clean and polluted marine boundary layers over the North Atlantic. J. Geophysical Res., 108(D6), 4189,

ACPD

11, 15775–15799, 2011

doi:10.1029/2002JD002106, 2003.
Li, W. and Shao, L.: Transmission electron microscopy study of aerosol particles from the brown hazes in northern China. J. Geophys. Res., 114, D09302, doi:10.1029/2008JD011285, 2009.
Mamani-Paco, R.: Morphology distributions and chemical composition of size-selected atmospheric fine particles. PhD dissertation, AAT 3156402, ISBN 0496171003, University of Connecticut, Storrs, CT, USA, 2004.
Márquez, C., Castro, T., Muhlia, A., Martínez-Arroyo, M. A., and Báez, A.: Measurement of aerosol particles, gases and flux radiation in the National Park Pico de Orizaba, and its relationship to air pollution transport. Atmos. Environ., 39, 21, 3877-3890, 2005.
Marley, N. A., Gaffney, J. S., Castro, T., Salcido, A., and Frederick, J.: Measurements of aerosol absorption and scattering in the Mexico City Metropolitan Area during the MILAGRO field campaign: a comparison of results from the T0 and T1 sites. Atmos. Chem. Phys., 9, 189–206, doi:10.5194/acp-9-189-2009, 2009
Molina, L. T. and Molina, M. J.: Air quality in the Mexico Megacity, An integrated assessment, Kluwer Academic, The Netherlands, 408 pp., 2002.
Molina, L. T., Madronich, S., Gaffney, J. S., Apel, E., de Foy, B., Fast, J., Ferrare, R., Herndon, S., Jiménez, J. L., Lamb, B., Osornio-Vargas, A. R., Russell, P., Schauer, J. J., Stevens, P. S., Volkamer, R., and Zavala, M.: An overview of the MILAGRO 2006 Campaign: Mexico City emissions and their transport and transformation, Atmos. Chem. Phys., 10, 8697–8760, doi:10.5194/acp-10-8697-2010, 2010.
Mogo, S., Cachorro, V. E., and De Frutos, A. M.: Morphological, chemical and optical absorbing characterization of aerosols in the urban atmosphere of Valladolid, Atmos. Chem. Phys., 5, 2739–2748, doi:10.5194/acp-5-2739-2005, 2005.
Okada, K. and Heintzenberg, J.: Size distribution, state of mixture, and morphology of urban aerosol particles at given electrical mobilities, J. Aerosol Sci., 34, 1539–1553, 2003.
Paredes-Miranda, G., Arnott, W. P., Jiménez, J. L., Aiken, A. C., Gaffney, J. S., and Marley, N. A.: Primary and secondary contributions to aerosol light scattering and absorption in Mexico City during the MILAGRO 2006 campaign, Atmos. Chem. Phys., 9, 3721–3730, doi:10.5194/acp-9-3721-2009, 2009.
Pósfai, M., Simonics, R., Li, J., Hobbs, P. V., and Buseck, P. R.: Individual aerosol particles from biomass burning in southern Africa: 1. Composition and distributions of carbonaceous particles.J. Geophys. Res., 108(D13), 8483, doi:10.1029/2002JD002291, 2003.

ACPD
11, 15775–15799, 2011

Raga, G., Baumgardner, D., Castro, T., Matínez-Arroyo, M. A., and Navarro-González, R.: Mexico City Air Quality: A Qualitative Review of Gas and Aerosol Measurements (1960-2000). Atmos. Environ., 35, 4041–4058, 2001.

Ramsden, A. R. and Shibaoka, M.: Characterization and analysis of individual fly-ash particles from coal-fired power stations by a combination of optical microscopy, electron microscopy and quantitative electron microprobe analysis, Atmos. Environ., 16(9), 2191–2206, 1982.

Salcedo, D., Onasch, T. B., Dzepina, K., Canagaratna, M. R., Zhang, Q., Huffman, J. A., De Carlo, P. F., Jayne, J. T., Mortimer, P. Worsnop, D. R., Kolb, C. E., Johnson, K. S., Zuberi, B., Marr, L. C., Volkamer, R., Molina, L. T., Molina, M. J., Cárdenas, B., Bernabé, R. M., Márquez, C., Gaffney, J. S., Marley, N. A., Laskin, A., Shutthanandan, V., Xie, Y., Brune, W., Lesher, R., Shirley, T., and Jiménez, J. L.: Characterization of ambient aerosols in Mexico City during the MCMA-2003 campaign with Aerosol Mass Spectrometry: results from the CENICA Supersite, Atmos. Chem. Phys., 6, 925–946, doi:10.5194/acp-6-925-2006, 2006.

Seinfeld, J. H. and Pandis, S. N.: Atmospheric chemistry and physics: from air pollution to climate change, John Wiley, New York, USA, 1326 pp., 1998.

Xiong, C. and Friedlander, S. K.: Morphological properties of atmospheric aerosol aggregates, Proc. Natl. Acad. Sci. USA, 98, 11851–11856, available online at: www.pnas.org/cgi/doi/10.1073/pnas.211376098, 2001.

ACPD

11, 15775–15799, 2011

Table 1. Absorption and scattering coefficients from three different sites.

Coefficient	T1	Pico de Orizaba	Mexico City
σ_{abs} (Mm^{-1})	28	17	22
σ_{sct} (Mm^{-1})	53	39	142

ACPD
11, 15775–15799, 2011

Table 2. Fractal dimension statistics for atmospheric particles analyzed on TEM.

Aerodynamic diameter = 0.18 µm								
	15 March				19 March			
	06:00	11:00	16:00	21:00	06:00	11:00	16:00	21:00
Number	36	32	56	51	54	44	37	50
Minimum	1.03	1.01	1.01	1.03	1.01	1.02	1.01	1.02
Maximum	1.31	1.21	1.25	1.25	1.31	1.26	1.25	1.27
Average	1.15	1.09	1.07	1.09	1.10	1.08	1.08	1.11
Standard dev	0.08	0.06	0.04	0.05	0.06	0.06	0.06	0.07

ACPD
11, 15775–15799, 2011

Table 3. Fractal dimension statistics for atmospheric particles analyzed on TEM.

Aerodynamic diameter = 1.8 µm								
	15 March				19 March			
	06:00	11:00	16:00	21:00	06:00	11:00	16:00	21:00
Number	42	65	61	31	41	32	47	33
Minimum	1.01	1.01	1.03	1.00	1.00	1.01	1.01	1.00
Maximum	1.23	1.16	1.19	1.18	1.20	1.32	1.24	1.18
Average	1.08	1.06	1.10	1.05	1.05	1.08	1.10	1.05
Standard dev	0.06	0.03	0.05	0.04	0.05	0.05	0.06	0.04

ACPD
11, 15775–15799, 2011

Table 4. Elemental composition of atmospheric particles (1.8 and 0.18 µm aerodynamic diameters) sampled on 15 and 19 March. Average results for particles analyzed on Fig. 3. Weight percent.

	15 March		19 March	
Element	1.8 µm	0.18 µm	1.8 µm	0.18 µm
C	5.8	21.7	3.9	77.9
O	15.7	4.6	18.4	11.1
Na	4.7		67.7	
Mg	2.2		3.5	
Al	5.3			
Si	19	6.1	0.3	9
P	0.9			
S	3.9		4.0	
K	1		0.6	1.1
Ca	38		0.6	
Fe	3.4	33.3		
Co		34.3		

ACPD
11, 15775–15799, 2011

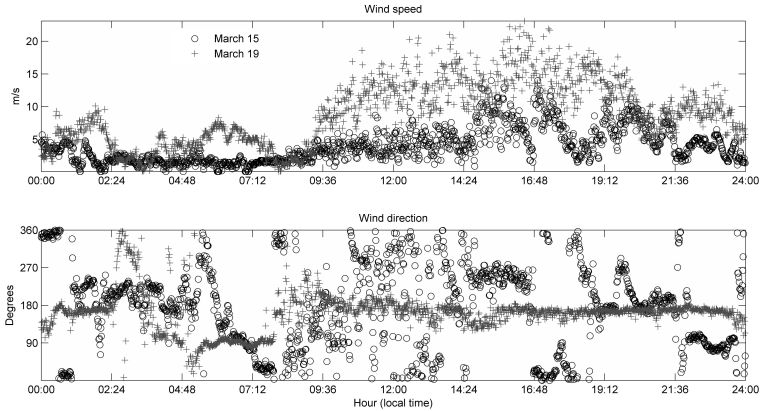

Fig. 1. Time series for wind speed and direction at T1 on 15 and 19 March.

ACPD
11, 15775–15799, 2011

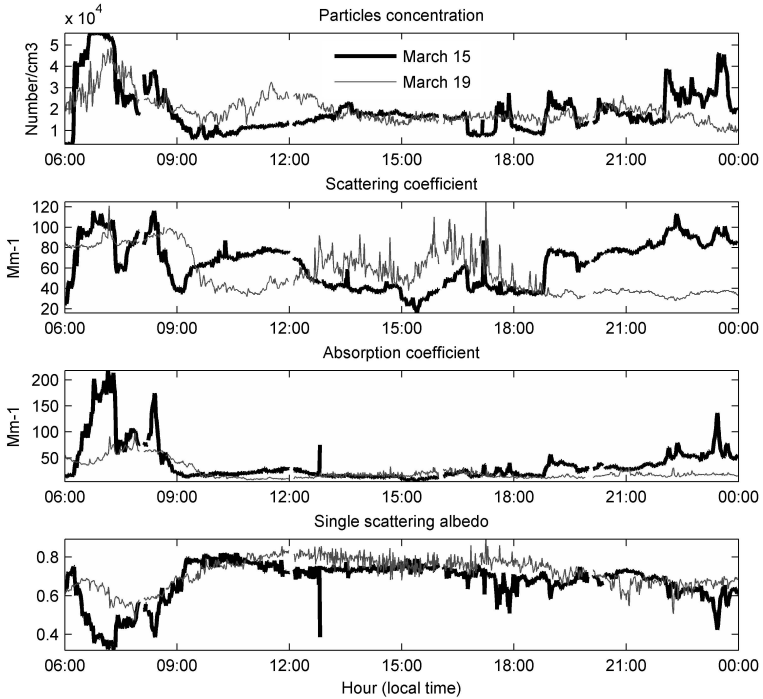

Fig. 2. Time series for particles concentration, absorption and scattering coefficients, and single scattering albedo for 15 and 19 March.

ACPD
11, 15775–15799, 2011

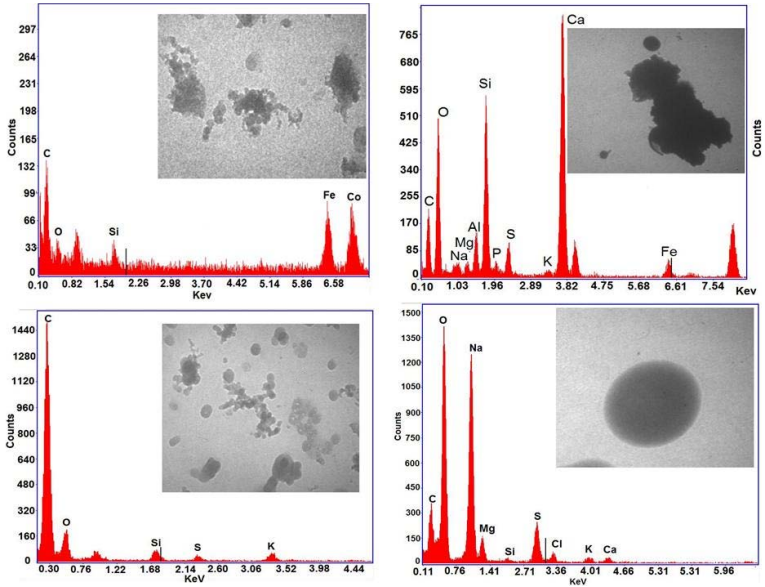

Fig. 3. TEM images and elemental analysis of atmospheric particles. Particles sampled on 15 March (row above) and 19 March (row below). Aerodynamic diameter 0.18 µm (column left) and 1.8 µm (column right).

ACPD
11, 15775–15799, 2011

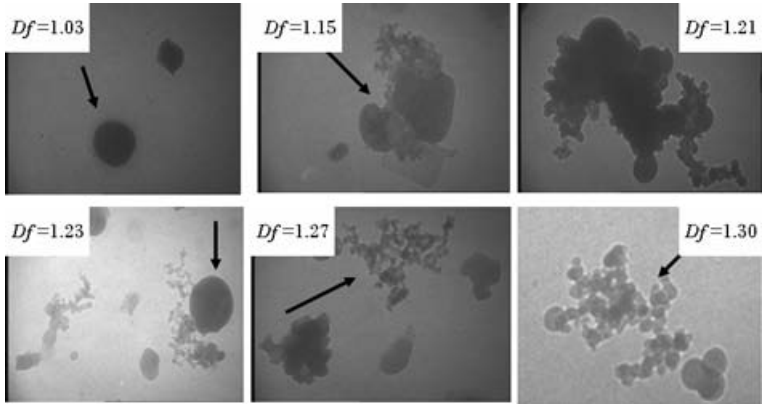

Fig. 4. TEM images with different dimension fractal (D_f) values of atmospheric particles, with 0.18 μm aerodynamic diameter.

ACPD
11, 15775–15799, 2011

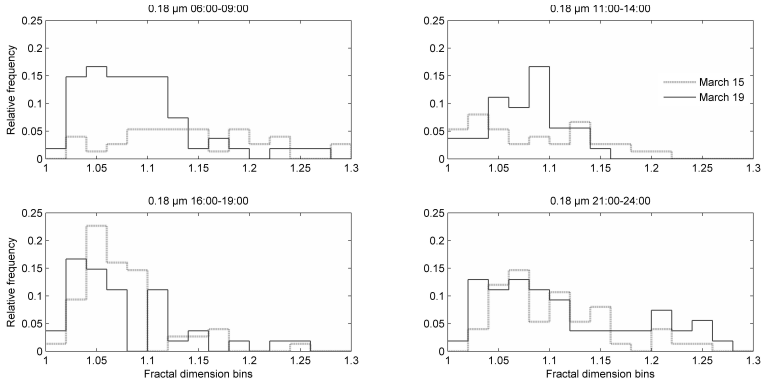

Fig. 5. Histograms of atmospheric particles (0.18 μm aerodynamic diameter), sorted by sampling time.

ACPD
11, 15775–15799, 2011

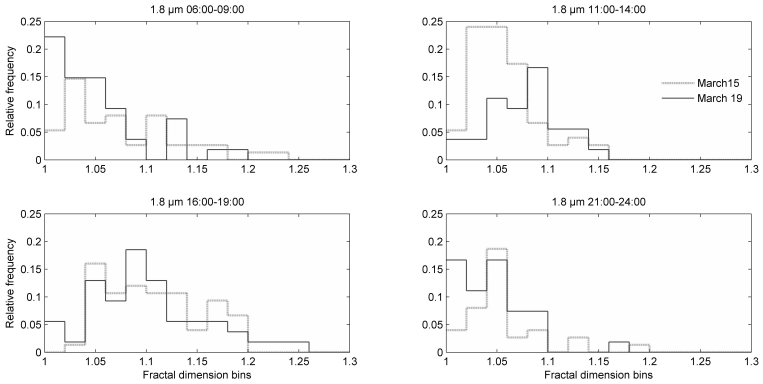

Fig. 6. Histograms of atmospheric particles (1.8 μm aerodynamic diameter), sorted by sampling time.

ACPD
11, 15775–15799, 2011